



Emission and cooling by CO in interstellar shock waves

D. Flower, A. Gusdorf

► To cite this version:

D. Flower, A. Gusdorf. Emission and cooling by CO in interstellar shock waves. Monthly Notices of the Royal Astronomical Society, 2009, 395 (1), pp.234-239. 10.1111/j.1365-2966.2009.14569.x . hal-02268218

HAL Id: hal-02268218

<https://hal.science/hal-02268218>

Submitted on 11 Jun 2021

HAL is a multi-disciplinary open access archive for the deposit and dissemination of scientific research documents, whether they are published or not. The documents may come from teaching and research institutions in France or abroad, or from public or private research centers.

L'archive ouverte pluridisciplinaire **HAL**, est destinée au dépôt et à la diffusion de documents scientifiques de niveau recherche, publiés ou non, émanant des établissements d'enseignement et de recherche français ou étrangers, des laboratoires publics ou privés.

Emission and cooling by CO in interstellar shock waves

D. R. Flower^{1★} and A. Gusdorf^{1,2†}

¹*Physics Department, The University, Durham DH1 3LE*

²*Institut d'Astrophysique Spatiale (IAS), Bâtiment 121, F-91405 Orsay, France*

Accepted 2009 January 28. Received 2009 January 15; in original form 2008 November 14

ABSTRACT

We have calculated emission by CO molecules from interstellar shock waves. Two approximations have been used to determine the population densities, n_J , of the rotational levels, J : steady state ($\partial/\partial t \equiv 0$) and statistical equilibrium ($d/dt \equiv 0$). A large-velocity-gradient approximation to the line-transfer problem was adopted in both cases. We find that there can be substantial differences between the values of the integrated rotational line intensities calculated in steady state and in the limit of statistical equilibrium. On the other hand, although CO can be the dominant coolant towards the rear of the cooling flow which follows the dynamical heating of the gas, the rate of cooling computed assuming statistical equilibrium is likely to be reasonably accurate, given that the limit of statistical equilibrium is approached in this region.

Key words: radiative transfer – shock waves – ISM: jets and outflows – ISM: molecules – infrared: ISM – radio lines: ISM.

1 INTRODUCTION

Carbon monoxide is one of the most widely observed and important molecules in the interstellar medium. After H_2 , it is the most abundant molecular species [$n(CO)/n(H_2) \approx 10^{-4}$], containing much of the elemental carbon. Because it is heavier than H_2 , CO has a smaller rotational constant [$B(CO) = 1.92 \text{ cm}^{-1}$, $B(H_2) = 59.3 \text{ cm}^{-1}$], and its lowest rotational transitions are readily observed from the ground at mm wavelengths. Higher rotational transitions, at shorter wavelengths, have been observed with the *Infrared Space Observatory* (ISO) satellite (Giannini, Nisini & Lorenzetti 2001). Being an ‘almost homonuclear’ molecule, CO has only a weak dipole moment (0.11 debye), and the radiative lifetime of its first rotationally excited level, $J = 1$, for example, is very large ($1.4 \times 10^7 \text{ s} = 0.44 \text{ yr}$). The small dipole moment inhibits the development of large optical depths in the rotational transitions, $J + 1 \rightarrow J$. However, owing to the large fractional abundance of CO, transitions between the lowest rotational levels, at least, become optically thick under the conditions in the interstellar medium. It follows that any modelling of the emission of CO, and the associated cooling, needs to incorporate a treatment of radiative line transfer.

In shock waves, the flow velocity of the gas changes more or less abruptly, depending on the physical conditions in the medium into which the shock propagates and the shock speed. Under these circumstances, it would be expected that the ‘large-velocity-gradient’ (LVG) approximation to radiative line transfer would be valid. This method was applied to the study of the cooling of warm molecular gas – such as is generated by the passage of a shock wave – by

Neufeld & Kaufman (1993). A more recent implementation of the LVG model of line transfer is the RADEX code of van der Tak et al. (2007).

The determination of the line optical depths requires the knowledge of the population densities of the energy levels; but the populations depend, in turn, on the line optical depths, as re-absorption of a line photon results in population transfer. Whilst the LVG approximation reduces the line-transfer problem to being local – the LVG implies that the line photons are absorbed ‘on the spot’ – it does not remove the mutual interdependence of the level populations and the line optical depths. In most implementations of the LVG approach, the level populations are assumed to be in statistical equilibrium (SE), and they are determined self-consistently with the line optical depths by means of iterative, algebraic methods. However, in dynamically active regions, where LVGs occur, other physical parameters, such as the density and the kinetic temperature, may also vary rapidly. Under these conditions, the assumption of SE when determining the level populations needs careful validation.

In this paper, we evaluate the emission and cooling by the CO molecule in interstellar shock waves, propagating in molecular gas. We compare results obtained using a conventional LVG code (Gusdorf et al. 2008a, hereafter G08a) with the predictions of a dynamical determination of the CO level populations and line intensities. Specifically, we integrate the equations for the population densities in parallel with the equations describing the evolution of the physical and chemical variables. This implementation not only eliminates the assumption of SE but obviates the need to solve iteratively for the level populations and the line optical depths. We find significant differences between predictions based on the conventional LVG method and the dynamical approach, as will be seen below.

In Section 2, we formulate our approach. Section 3 contains the numerical applications and comparisons and, in Section 4, we make our concluding remarks.

★E-mail: david.flower@durham.ac.uk

†Present address: Max Planck Institute für Radioastronomie Auf dem Hügel, D-53121, Bonn, Germany.

2 FORMULATION

The equations describing the temporal evolution of the level populations may be written as

$$\frac{dn_J}{dt} = \sum_{J'} n_{J'} R(J' \rightarrow J) - n_J \sum_{J'} R(J \rightarrow J'), \quad (1)$$

where n_J is the population density (cm^{-3}) of rotational level J and $R(J' \rightarrow J)$, $R(J \rightarrow J')$ are the total rates (s^{-1}) of population transfer from and to other rotational levels, J' . Transfer of population is induced by collisional and radiative processes. The principal collision partners are ortho- and para- H_2 , H and He, of which H_2 and H are dominant under the conditions of the models considered below. Radiative excitation and deexcitation occur through absorption and emission of photons at the frequencies of the rotational lines. The photon field is generated by collisional excitation of the molecule, followed by radiative decay, and there is a 'background' field, which, in practice, is taken to be the cosmic blackbody radiation at temperature $T_{\text{bb}} = 2.73 \text{ K}$. When the assumption of SE is made, the left-hand side of equation (1) is set equal to zero, leaving a set of homogeneous, first-order algebraic equations for the level population densities, which are complemented by the closure relation

$$n(\text{M}) = \sum_J n_J, \quad (2)$$

which states that the number density of molecular species M is the sum of the population densities of its rotational levels.

The equation of radiative transfer of the line photons takes the form

$$\frac{dI_\nu}{d\tau_\nu} = -I_\nu + S_\nu, \quad (3)$$

where I_ν is the local radiation intensity at frequency ν , τ_ν is the optical depth at this frequency and S_ν is the source function. We consider one-dimensional models, and τ_ν is the optical depth in this dimension, z , taken to be the direction of propagation of the shock wave. The expression for the source function is

$$S_\nu = \frac{2h\nu^3}{c^2} \frac{1}{\frac{n_J/g_J}{n_{J'}/g_{J'}} - 1}, \quad (4)$$

where h is Planck's constant and c is the velocity of light; $g_J = 2J + 1$ and $g_{J'} = 2J' + 1$ are the degeneracies of the rotational levels J and J' . As we consider only dipole transitions, the upper level $J' = J + 1$. The dependence of the source function on the level population densities is explicit in equation (4). If the LVG assumption is made, the transfer equation (3) may be integrated to yield

$$I_{\nu_0} = S_{\nu_0}(1 - e^{-\tau_{\nu_0}}) + B_{\nu_0}(T_{\text{bb}})e^{-\tau_{\nu_0}}, \quad (5)$$

where ν_0 is the frequency at the line centre and B_ν is the Planck (blackbody) function. The probability of escape of a photon, of frequency ν_0 , from the region in which it is produced is

$$\beta = \frac{1 - e^{-\tau_{\nu_0}}}{\tau_{\nu_0}}, \quad (6)$$

although other forms have been suggested in the literature. In particular, Neufeld & Kaufman (1993) proposed

$$\beta = \frac{1}{1 + 3\tau_{\nu_0}} \quad (7)$$

for the angle-averaged probability, in the case of a plane-parallel model, where τ_{ν_0} is evaluated along the direction of the flow (i.e. perpendicular to the shock front). We shall compare below re-

sults obtained using both expressions for the escape probability, (6) and (7), when calculating the level population densities. Given that the line photons are emitted in random directions, we consider the use of equation (7) to be more appropriate when evaluating the level populations. On the other hand, when calculating the line temperatures, the escape probability along the line of sight should be used, although its inclination to the direction of propagation of the shock wave is often unknown or uncertain, in practice. For the purposes of the comparison of results obtained using the SE and steady-state (SS) approximations, we have adopted equation (6) systematically when evaluating the line temperatures. Equation (6) is the escape probability along the direction of propagation of the shock wave, and also in the isotropic case.

An approximation which is superior to the assumption of SE ($d/dt \equiv 0$) when solving equation (1) is that of SS ($\partial/\partial t \equiv 0$). Then, $d/dt = v/dz$, where v is the fluid flow velocity in the z -direction, and equation (1) takes the form of an ordinary, first-order differential equation, in which there appear, on the right-hand side, the dependent variables: dynamical, chemical and the rotational level populations themselves. Such differential equations may be integrated in parallel by means of the method for solving 'stiff' ordinary differential equations developed originally by Gear (1971) and subsequently by A. C. Hindmarsh and his colleagues. The most recent implementation of this method is DVOLE (https://computation.llnl.gov/casc/odepack/odepack_home.html). By means of this technique, the level populations can be determined simultaneously with the physical and chemical variables, and iterative methods become redundant. The closure relation (2) was incorporated explicitly into the solutions, thereby ensuring conservation of the total CO population density. We note that Neufeld & Kaufman (1993) also integrated equation (1) by means of the Gear (1971) method; but they used this technique to determine the level populations at large times, when SE is attained, and not to determine the evolution of the level populations in parallel with the other dependent variables of the model, as is done here.

As is shown in appendix A of G08a, the intensity of radiation at frequency ν in a given rotational line, observed using the background subtraction technique, is

$$I_{\text{obs}}(\nu) = [B_\nu(T_{\text{ex}}) - B_\nu(T_{\text{bb}})](1 - e^{-\tau_\nu}), \quad (8)$$

where T_{ex} is the excitation temperature. The line radiation temperature is defined as

$$T_{\text{R}} \equiv \frac{I_{\text{obs}}c^2}{2k_B\nu^2}, \quad (9)$$

in which k_B is the Boltzmann constant and the integrated line temperature (in K km s^{-1}) is obtained by integrating T_{R} with respect to the flow speed of the neutral fluid, $v(z)$.

As shown by Elitzur & Watson (1978), when SE applies, the population densities of successive rotational levels J and $J + 1$ are related by

$$\frac{n_{J+1}}{n_J} = \frac{C_{J,J+1}}{C_{J+1,J} + A_{J+1,J}}$$

for an optically thin transition $J + 1 \rightarrow J$. In this equation, $A_{J+1,J}$ is the spontaneous radiative transition probability and the collisional rates are connected through the detailed balance relation,

$$(2J + 1)C_{J,J+1} = (2J + 3)C_{J+1,J} \exp[-(E_{J+1} - E_J)/k_B T],$$

where E denotes the energy of the level and T is the kinetic temperature. For electric dipole transitions, $A_{J+1,J} \propto (E_{J+1} - E_J)^3$ and $E_{J+1} - E_J \approx 2B(J + 1)$, where B is the rotational constant. The rate

of collisional deexcitation, $C_{J+1,J}$, is approximately independent of J .

3 RESULTS AND DISCUSSION

The validity of the assumption of SE is usually assessed by comparing the time-scale for population transfer by collisions with a dynamical time-scale, determined by the conditions of the flow. In the case of a shock wave, the latter may be taken to be the flow time of the neutral fluid through the relevant part of the shock wave. For the former time-scale, one might take $[n(\text{H}_2)q(J+1 \rightarrow J)]^{-1}$, where $q(J+1 \rightarrow J)$ is the rate coefficient for transfer of population between adjacent rotational levels through collisions with hydrogen molecules; $q(J+1 \rightarrow J) \approx 10^{-10} \text{ cm}^3 \text{ s}^{-1}$ is a representative numerical value, at kinetic temperatures of a few 100 K, believed to be appropriate to many interstellar shock waves. Taking $n(\text{H}_2) = 10^4 \text{ cm}^{-3}$ for the density of the molecular gas yields a time-scale for population transfer of $10^6 \text{ s} = 0.03 \text{ yr}$. Given that this value is smaller, or much smaller, than typical flow times, it is tempting to conclude that the assumption of SE is valid. However, as we shall show, this conclusion is not necessarily correct.

In the cold, pre-shock gas, CO is found predominantly in its lowest rotational states. As the kinetic temperature increases, due to heating by the shock wave, more highly excited rotational states become populated through inelastic collisions, principally with H_2 and H . This process involves climbing the ladder of rotational energy levels, mainly in single-level steps ($J \rightarrow J+1$). Thus to populate level $J+10$ from level J requires 10 successive steps, enhancing the corresponding time-scale by an order of magnitude to 0.3 yr; but there is an additional effect acting which substantially increases the time-scale for population transfer up the rotational ladder. By level $J=3$, the probability of spontaneous radiative decay, $A(3 \rightarrow 2) = 2.5 \times 10^{-6} \text{ s}^{-1}$, already exceeds the probability of collisional transfer upwards, to $J=4$, for the conditions adopted above. The A values continue to increase with J and approach 10^{-3} for $J=20$. It follows that less than 1 per cent of the population transferred by collisions from $J=17$ to 18, for example, is available for subsequent transfer to $J=19$. We conclude that the time-scale for population transfer to such highly excited rotational levels is typically of the order of 100 yr, which is comparable with the dynamical time-scale, as will be seen below. If the collisional rate coefficients are (artificially) enhanced by a factor of 100, the delay in populating the excited states, following the temperature rise, practically disappears, as we have verified numerically.

We shall compare first the numerical results obtained for representative C-type (continuous), and J-type (jump) shock models, and then for a CJ-type model, which incorporates both a J-discontinuity and a magnetic precursor.

3.1 C-type shocks

We consider a C-type shock wave of speed $v_s = 30 \text{ km s}^{-1}$, propagating into gas of density $n_{\text{H}} \equiv n(\text{H}) + 2n(\text{H}_2) = 10^5 \text{ cm}^{-3}$; the initial value of the transverse magnetic field strength is $B = 200 \mu\text{G}$. These parameters are representative of shocks in molecular outflows. In Fig. 1, the fractional population densities, $n_J/n(\text{CO})$, of a sample of the rotational levels of CO, $J=0, 6, 12, 16$, are plotted, in both the SE and SS approximations.

Fig. 1 demonstrates that the approximation of SE leads to the population densities of the highly excited rotational levels, such as $J=12$ and 16, being overestimated immediately beyond the

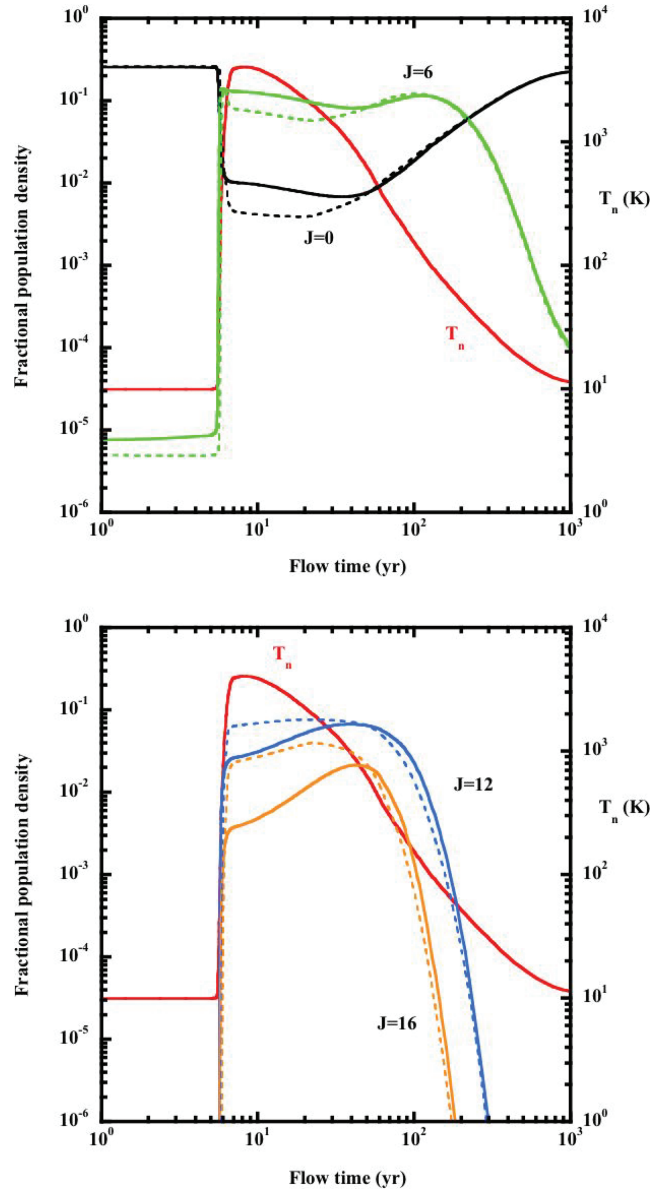


Figure 1. The fractional population densities, $n_J/n(\text{CO})$, of the rotational levels $J=0, 6, 12, 16$ of CO, as functions of the flow time of the neutral fluid through a C-type shock wave; see Section 3.1. In the upper panel are plotted $J=0$ and 6; in the lower panel, $J=12$ and 16. The SS solutions are the full curves, the SE solutions are the broken curves. The temperature of the neutral fluid, T_n , is plotted in both panels. Results are shown for $v_s = 30 \text{ km s}^{-1}$, $n_{\text{H}} = 10^5 \text{ cm}^{-3}$, $B = 200 \mu\text{G}$.

region in which the initial rise in the temperature of the neutral fluid takes place. In effect, there is a delay in populating such excited states, in response to the rise in temperature, compared with the predictions of SE. Following the discussion above, and allowing for the higher pre-shock density [$n(\text{H}_2) = 10^5 \text{ cm}^{-3}$] of the model illustrated in Fig. 1, we expect the time-scale for populating the high rotational levels, following the temperature rise, to be of the order of 10 yr, whereas the temperature increases in a flow time of approximately 1 yr. Subsequently, as the temperature begins to fall and the gas to be compressed (thereby reducing the time-scale for collisional population transfer), the solutions in the two cases become indistinguishable, as may be seen in Fig. 1.

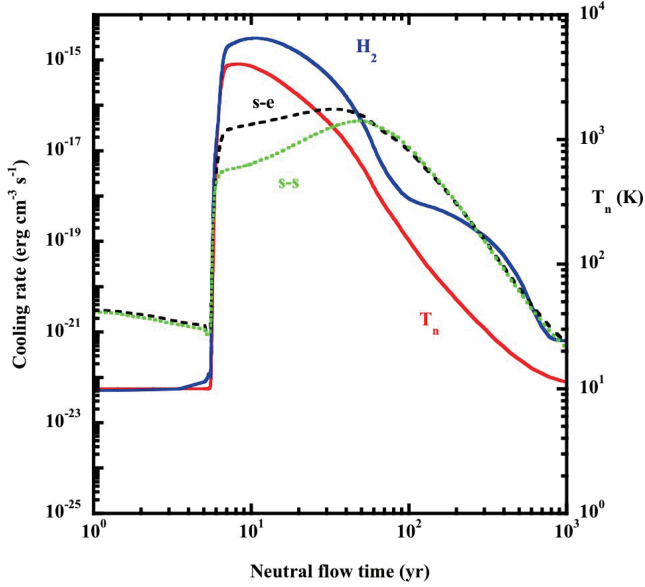


Figure 2. The rates of cooling per unit volume by CO, as predicted by the SE and the SS approximations, and by H₂, for the same shock model as in Fig. 1: $v_s = 30 \text{ km s}^{-1}$, $n_H = 10^5 \text{ cm}^{-3}$, $B = 200 \text{ } \mu\text{G}$. The temperature of the neutral fluid, T_n , is shown also.

We mentioned in the Introduction that one of the motivations for studying the emission by CO is its potential significance as a coolant; this is especially true in shock waves, owing partly to the collisional dissociation of molecular hydrogen in the hot gas, but mainly to the large rotational constant of H₂, which causes the rates of collisional excitation of its rotational levels to decrease rapidly at temperatures below about 500 K.

In Fig. 2, we show the rates of cooling per unit volume by CO, as predicted by the SE and the SS approximations, and by H₂. The cooling rate was evaluated as the rate of removal of kinetic energy from the gas, the difference of collisional excitation (kinetic energy loss) and deexcitation (kinetic energy gain) processes:

$$\sum_J (n_J C_{J,J+1} - n_{J+1} C_{J+1,J}) (E_{J+1} - E_J).$$

We emphasize that, as above, the results refer to the *same* shock model, and, in particular, the differences in the CO cooling rate have not been fed back into the calculation of the thermal profile, which remains identical in the two cases. As might have been anticipated from the comparison of the level populations, the SE solution overestimates, by approximately an order of magnitude, the rate of CO cooling in the region immediately beyond the temperature rise. The two calculations of the rate of cooling by CO become identical subsequently, as the gas cools and is compressed. Cooling by H₂ dominates initially but then falls below that of CO as the temperature decreases. However, by the time that the CO cooling comes to exceed that by H₂, the two calculations of the CO cooling rate have converged.

3.2 J-type shocks

It might be anticipated that the significance of the delay in transferring population up the CO rotational ladder would be greater behind the ‘discontinuity’ in J-type shock waves, at which the temperature rise is much more rapid than in C-type shock waves. Accordingly, we compared the fractional populations of the CO rotational lev-

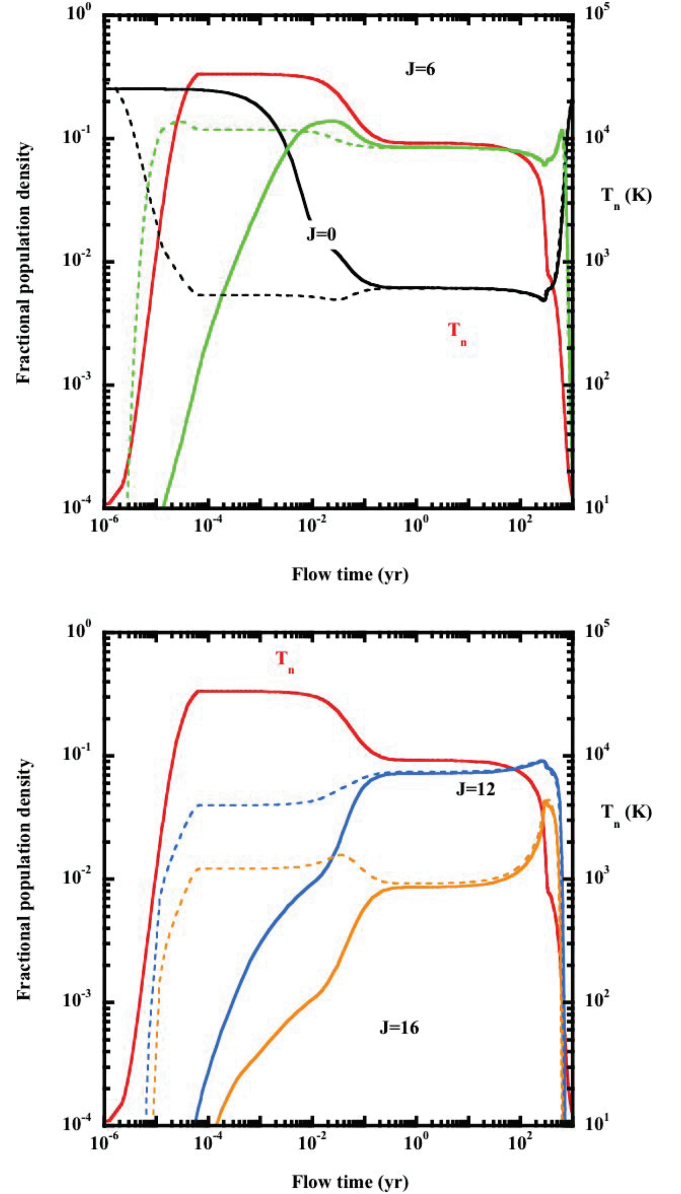


Figure 3. The fractional population densities, $n_J/n(\text{CO})$, of the rotational levels $J = 0, 6, 12, 16$ of CO, as functions of the flow time of the fluid through a J-type shock wave; see Section 3.2. In the upper panel are plotted $J = 0$ and 6; in the lower panel, $J = 12$ and 16. The SS solutions are the full curves, the SE solutions are the broken curves. The temperature of the neutral fluid, T_n , is plotted in both panels. Results are shown for $v_s = 25 \text{ km s}^{-1}$, $n_H = 10^4 \text{ cm}^{-3}$ and $B = 10 \text{ } \mu\text{G}$ (see the text, Section 3.2).

els, in SE and SS, for a J-type (single-fluid) model in which $v_s = 25 \text{ km s}^{-1}$, $n_H = 10^4 \text{ cm}^{-3}$ and $B = 10 \text{ } \mu\text{G}$. Our expectation is seen to be justified only partially by the numerical results in Fig. 3. The time delay between the SE and SS solutions is of the order of 1 yr, which is less than the estimate of 10^2 yr made above, for the pre-shock density $n_H = 10^4 \text{ cm}^{-3}$ of this model. A combination of factors results in the reduced delay time: the compression of the gas (by a factor of 4) at the J-‘discontinuity’, which continues into the cooling flow; the high kinetic temperature behind the ‘discontinuity’, which enhances the collisional excitation rates; and the dissociation of H₂ to H, which leads to a higher perturber density [$n(\text{H}) = n_H$ in atomic gas, whereas $n(\text{H}_2) = n_H/2$ in molecular gas.

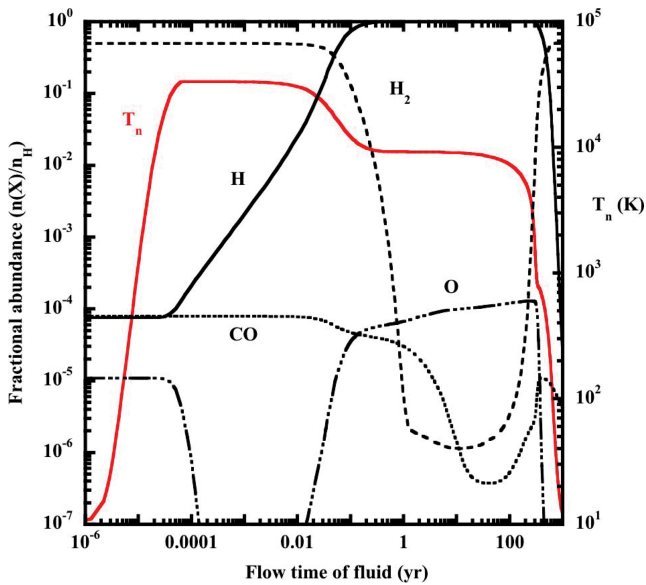


Figure 4. Illustrating the collisional dissociation of H_2 and the chemical dissociation of CO, in the reaction $\text{H}(\text{CO}, \text{OH})\text{C}$, which is followed by $\text{H}(\text{OH}, \text{H}_2\text{O})$; both these reactions are rapid in the hot gas, where the hydrogen is mainly in atomic form. The J-‘discontinuity’ is smoothed numerically by means of an artificial viscosity (see the text, Section 3.2). Results are shown for $v_s = 25 \text{ km s}^{-1}$, $n_{\text{H}} = 10^4 \text{ cm}^{-3}$ and $B = 10 \text{ } \mu\text{G}$.

Furthermore, the rate coefficients for rotationally inelastic collisions of CO with H are larger than for collisions with H_2 by a factor of typically 3–4.]

Once again, however, the effects on the thermal balance of the medium are mitigated by the high post-shock temperature, which enhances the rate of cooling by molecular hydrogen. Although H_2 is collisionally dissociated in the hot gas behind the ‘discontinuity’, CO is dissociated chemically in this region, owing to the reaction $\text{H}(\text{CO}, \text{OH})\text{C}$, which is rapid at high temperatures; see Fig. 4. Consequently, cooling by H_2 dominates.

It should be noted that, in the models of J-type shock waves, the J-‘discontinuity’ is smoothed numerically, by introducing an artificial viscosity; see Flower et al. (2003).

3.3 CJ-type shocks

In a recent study (Gusdorf et al. 2008b, hereafter G08b), we modelled the emission of H_2 , SiO and CO from shocks in molecular outflows, particularly L1157 B1. We confirmed a result of earlier work, which showed that, in order to fit the observations of the rotational and rovibrational lines of H_2 , CJ-type models, which comprise a magnetic precursor and a J-discontinuity, are necessary. The discontinuity is introduced at a specified value of the flow time of the charged fluid, identified with the evolutionary age of the shock wave (see G08b, appendix C).

In Fig. 5, we compare the integrated CO line temperatures (K km s^{-1}) predicted by the two approximations to the CO level populations, SE and SS. The upper panel of Fig. 5 contains the results of the two models which define the envelope of the results plotted in fig. B.1 of G08b: a shock speed $v_s = 20 \text{ km s}^{-1}$, pre-shock density $n_{\text{H}} = 10^4 \text{ cm}^{-3}$ and the pre-shock magnetic field strengths, B , and shock ages, t_s , specified in the figure. The ISO observations of the blue lobe of L1157 (Giannini et al. 2001) are plotted also. The lower panel of Fig. 5 contains the corresponding SS results.

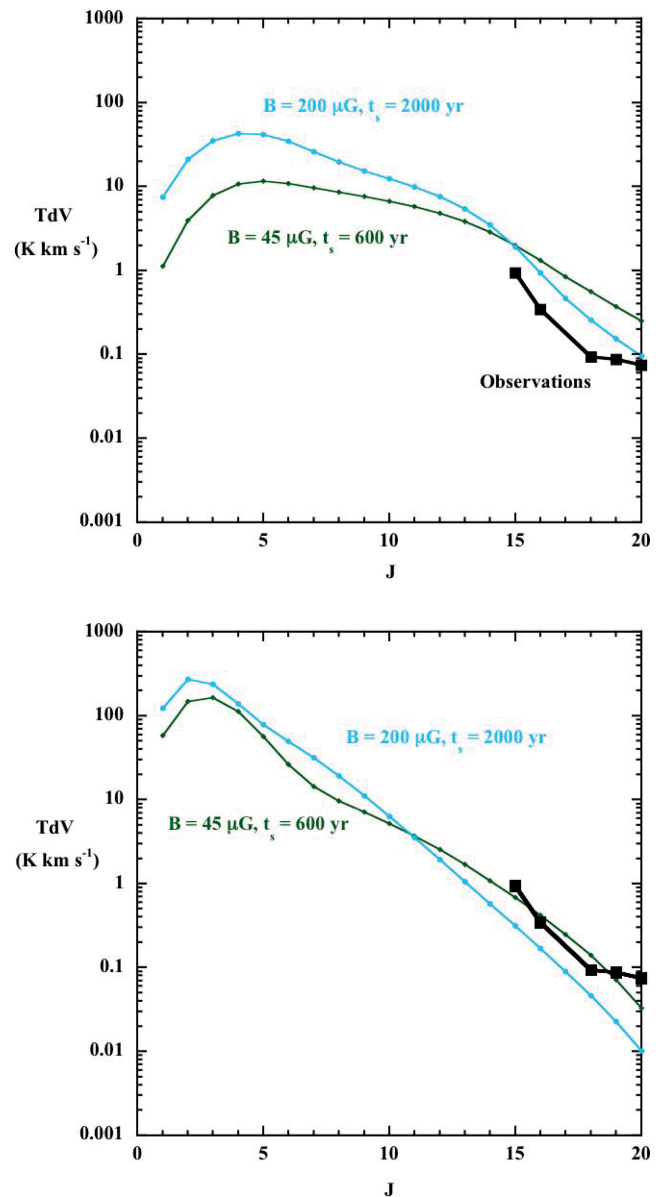


Figure 5. The integrated line CO rotational intensities, TdV (K km s^{-1}), predicted in the SE (upper panel) and SS (lower panel) approximations. Results are shown for two models: $v_s = 20 \text{ km s}^{-1}$, $n_{\text{H}} = 10^4 \text{ cm}^{-3}$, $B = 200 \text{ } \mu\text{G}$ and $t_s = 2000 \text{ yr}$ (full blue circles), $B = 45 \text{ } \mu\text{G}$ and $t_s = 600 \text{ yr}$ (full green lozenges; see the text, Section 3.3). The observations of L1157 B1 compiled by Giannini et al. (2001) are plotted in both panels as full black squares.

Fig. 5 shows that, whilst the variation of the line intensities with the emitting rotational level, as predicted by the two approximations, is broadly similar, the differences between them are nonetheless significant. In the limit of SE, both models yield line intensities which exceed those observed for $15 \leq J \leq 20$, whereas the SS results pass through or fall somewhat below the observed points. G08b commented that these high- J observations provide inadequate discrimination between the models. Unfortunately, combining high- J (satellite) and low- J (ground-based) observations of L1157 (Giannini et al. 2001; Hirano & Taniguchi 2001) involves using measurements made with different instruments and beam sizes and is consequently a non-trivial task.

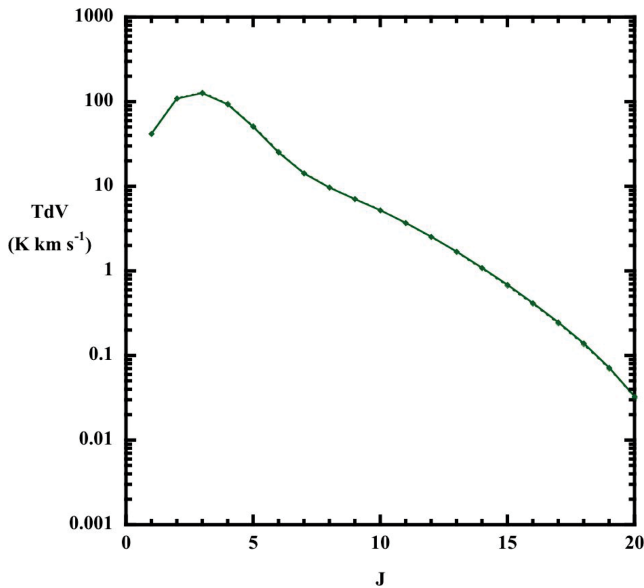


Figure 6. A comparison of the integrated line CO rotational intensities, Tdv (K km s^{-1}), predicted in SS, using different expressions for the escape probability: equation (6) (broken curve); equation (7) of Neufeld & Kaufman (1993) (full curve); the two curves appear superposed. Results are shown for the CJ-type model in which $v_s = 20 \text{ km s}^{-1}$, $n_H = 10^4 \text{ cm}^{-3}$, $B = 45 \text{ } \mu\text{G}$ and $t_s = 600 \text{ yr}$ (see the text, Section 3.3).

We mentioned in Section 2 that different expressions have been suggested for the line escape probability. In Fig. 6, the results obtained for the specified CJ-type model are compared, using either equation (6) or (7) [of Neufeld & Kaufman (1993)] for the escape probability. We see that the form adopted for the escape probability has negligible consequences for the line intensities: the populations of the lower rotational levels are thermalized by collisions, whereas transitions from higher levels are optically thin.

4 CONCLUDING REMARKS

We have investigated the implications for interstellar shock waves of the finite time which is required to populate by collisions the excited rotational states of the CO molecule. We find that there is a significant delay in populating the highly excited states in both J- and C-type shock waves. In CJ-type shock waves, which are believed to be relevant to the emission from dynamically young flows, such as L1157, allowance for the finite flow speed has consequences for the predicted values of the integrated rotational line intensities over the entire range of quantum number ($0 \leq J \leq 20$) that we considered.

Carbon monoxide was selected for study because of its importance as a coolant of molecular gas. In practice, our calculations suggest that departures from SE have limited consequences for the rate of cooling of the medium. Although CO can become the principal coolant in shock waves, as the kinetic temperature falls, following the initial dynamical heating, the CO cooling rate has become, by this point in the flow, almost the same in SS as in the limit of SE.

The results presented here for CO beg the question of the importance of departures from SE in the case of SiO, studied by G08a,b, and so we have performed separate calculations to investigate the significance of these effects in the context of SiO emission. Owing to the lower elemental abundance of silicon, relative to carbon, SiO is not a significant coolant of the medium. The dipole moment of SiO in its ground vibrational state (3.1 debye) is much larger than that of CO, and the radiative transition probabilities of the corresponding transitions, $J + 1 \rightarrow J$, in SiO are approximately 40 times larger than in CO. As a consequence of the larger radiative transition probabilities, the time-scale for climbing the rotational ladder of SiO is larger than for CO; the optical depths in the lines of SiO tend to be larger also. G08a,b considered rotational transitions in SiO up to $11 \rightarrow 10$, as observed by Nisini et al. (2007). Owing to the larger reduced mass of SiO, the level $J = 11$ lies only 138 K above the $J = 0$ ground state, as compared with 365 K in CO. Thus, the emission from SiO tends to arise from the compressed and relatively cold gas, towards the rear of the cooling flow of the shock wave. This tendency is reinforced by the chemical delay associated with the formation of SiO in the gas phase, if it forms by oxidation of Si that is released by the sputtering of silicate grains (cf. Gusdorf et al. 2008a). As a consequence, departures from SE prove to be less important for the emission of SiO than CO. On the other hand, the integrated intensities of the rotational transitions of SiO are more sensitive to the form adopted for the escape probability (equation 6 or 7).

ACKNOWLEDGMENTS

Antoine Gusdorf and the University of Durham acknowledge the support of the European Commission under the Marie Curie Research Training Network ‘The Molecular Universe’ MRTN-CT-2004-512302. We thank the referee for some perceptive comments.

REFERENCES

- Elitzur M., Watson W. D., 1978, *A&A*, 70, 443
- Flower D. R., Le Bourlot J., Pineau des Forêts G., Cabrit S., 2003, *MNRAS*, 341, 70
- Gear C. W., 1971, *Numerical Initial Value Problems in Ordinary Differential Equations*. Prentice-Hall, Englewood Cliffs, NJ
- Giannini T., Nisini B., Lorenzetti D., 2001, *ApJ*, 555, 40
- Gusdorf A., Cabrit S., Flower D. R., Pineau des Forêts G., 2008a, *A&A*, 482, 809 (G08a)
- Gusdorf A., Pineau des Forêts G., Cabrit S., Flower D. R., 2008b, *A&A*, 490, 695
- Hirano N., Taniguchi Y., 2001, *ApJ*, 550, L219
- Neufeld D. A., Kaufman M. J., 1993, *ApJ*, 418, 263
- Nisini B., Codella C., Giannini T., Santiago Garcia J., Richer J. S., Bachiller R., Tafalla M., 2007, *A&A*, 462, 163
- van der Tak F. F. S., Black J. H., Schöier F. L., Jansen D. J., van Dishoeck E. F., 2007, *A&A*, 468, 627

This paper has been typeset from a \LaTeX file prepared by the author.